ELSEVIER

Journal of Alloys and Compounds 388 (2005) 1–5

Journal of ALLOYS AND COMPOUNDS

www.elsevier.com/locate/jallcom

Metal–insulator transition and large thermoelectric power of a layered palladium oxide: $PbPdO_2$

T.C. Ozawa[a,*], T. Taniguchi[a], Y. Nagata[a], Y. Noro[b],
T. Naka[c], A. Matsushita[c]

[a] *College of Science and Engineering, Aoyama Gakuin University, Fuchinobe, Sagamihara, Kanagawa 229-8558, Japan*
[b] *Kawazoe Frontier Technologies, Co. Ltd. Kuden, Sakae, Yokohama, Kanagawa 931-113, Japan*
[c] *National Institute for Materials Science, Ibaraki 305-0047, Japan*

Received 31 May 2004; received in revised form 22 June 2004; accepted 22 June 2004

Abstract

Single-phase polycrystalline samples of $PbPdO_2$ have been synthesized via solid-state reaction, and their electrical, magnetic and thermoelectric properties have been characterized. The temperature-dependent dc electrical resistivity exhibits metal–insulator transition around 90 K. Thermoelectric power and Hall effect measurement results indicate that the majority of carriers in $PbPdO_2$ are holes. The thermoelectric power is 95 μV/K at 290 K and large for metallic materials. Based on the temperature proportionality of thermoelectric power, $PbPdO_2$ is essentially a metal. The insulating behavior at low temperatures is driven by localization of charge carriers manifested by Curie paramagnetism.

Keywords: Metal–insulator transition; Thermoelectric power; Magnetic property; Electrical property; Hall effect

1. Introduction

Since the discovery of high-temperature superconductivity in layered cuprates [1], there has been a great deal of interest in layered metal oxides, and numerous new properties have been discovered in them. For examples, superconductivity in non-cuprate layered oxides such as Sr_2RuO_4 [2] and $Na_xCoO\cdot yH_2O$ [3], and large thermoelectric power in $NaCo_2O_4$ [4] have recently been reported. Thus, physical property characterization of various layered oxide materials are under scrutiny. Among the transition metal oxides, palladium oxides are of particular interest because they tend to form square planar $[PdO_{4/2}]^{2-}$ unit analogous to a fundamental unit of cuprate superconductors, $[CuO_{4/2}]^{2-}$. For example, Sr_2PdO_3 is isostructural to a layered cuprate, Sr_2CuO_4, except for the oxygen deficiency [5]. Therefore, palladium oxides are interesting objects for the investigation of structure–property relationship. In addition, palladium in oxide compounds prefers to have oxidation states of 2+ and 4+ rather than 3+ [6]. When holes are doped to a compound containing Pd^{2+}, holes prefer to pair up and locate on the same Pd site forming Pd^{4+} rather than forming Pd^{3+} at different sites [7]. Induction of superconductivity is expected when such a valence skipper is carrier doped [8] as in the case of Bi in $BaPb_{1-x}Bi_xO_3$ [9] and $Ba_{1-x}K_xBiO_3$ [10]. From these points of view, a layered palladium oxide, $PbPdO_2$ is an interesting compound to investigate its physical properties. The structure of $PbPdO_2$ is shown in Fig. 1. $PbPdO_2$ consists of corrugated Pd–O layers stacked along *a*-axis [11]. In the Pd–O layer, Pd is four coordinated by oxygens in square planar configuration, and this $[PdO_{4/2}]^{2-}$ unit is corner shared to form layers extending in *b*–*c* plane. These layers are bridged by Pb which is four coordinated by oxygens in square pyramid configuration, $[PbO_{4/2}]^{2-}$. This coordination configuration is familiar in lower group 14 metal oxides such as α-PbO

---

[*] Corresponding author.
E-mail address: tcozawa@ee.aoyama.ac.jp (T.C. Ozawa).

0925-8388/$ – see front matter © 2004 Elsevier B.V. All rights reserved.
doi:10.1016/j.jallcom.2004.06.089

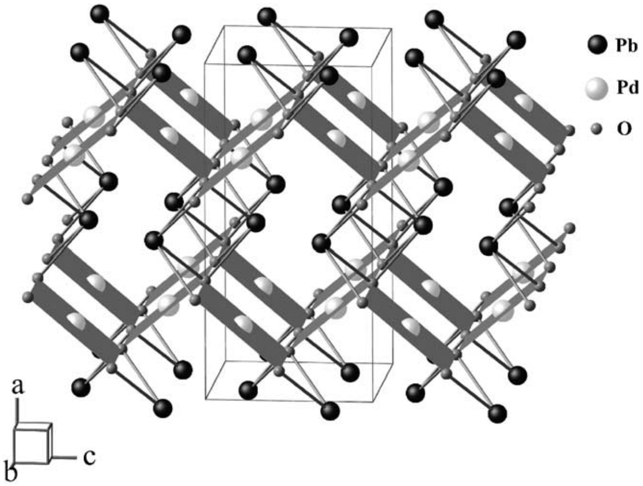

Fig. 1. Crystal structure of $PbPdO_2$. Gray squares indicate $[PdO_{4/2}]^{2-}$ square planar units.

(litharge) [12] and SnO [13]. Temperature-dependent resistivity of $PbPdO_2$ in the range of 90–300 K have previously been reported by Watanabe and Nozaki [14], and their results indicate that $PbPdO_2$ has metallic conductivity in this temperature range. However, physical properties of $PbPdO_2$ below 90 K are not known. In this paper, we extended the resistivity measurement down to 5 K. In addition, magnetic susceptibility, Hall effect and thermoelectric properties of $PbPdO_2$ have been characterized.

2. Experiment

Polycrystalline samples of $PbPdO_2$ were prepared by solid-state reaction of β-PbO (massicot, 99.999%) and PdO (99.9%). Stoichiometric amounts of PbO and PdO powders plus 2 mol% excess of PbO powder were weighed. The extra amount of PbO is to account for the volatility of PbO at high temperature. The weighed powders were mixed thoroughly in an agate mortar and the resulting mixture was pressed into a pellet. The pellet was heated at 700 °C in air for a few days with several intermittent grindings.

Powder X-ray diffraction data were acquired on a Shimadzu XRD-6000 (Cu Kα radiation). Crystal structure analysis was performed by the Rietveld method using RIETAN-2000 [15]. Magnetic susceptibility measurements were performed with a Quantum Design $MPMS_2$ SQUID magnetometer in the range of 5–300 K in a 1 T field. The electrical resistivity was measured in a helium-cooled cryostat in the range of 5–290 K. Gold leads were attached to the specimen by gold paste, and data were acquired by a four-probe method. Thermoelectric power was measured by a dc steady-state method in the range of 10–290 K. The thermoelectric contribution of the voltage leads was carefully subtracted. Hall effect was measured in the range of 5–290 K using a Quantum Design PPMS under applied magnetic field range of −8 to 8 T.

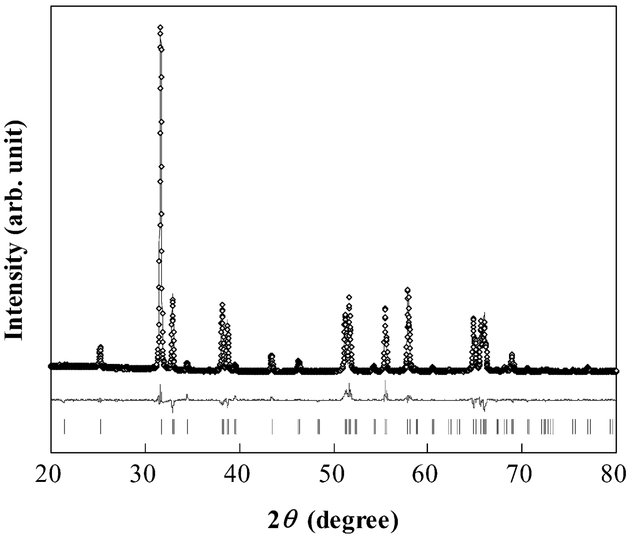

Fig. 2. Observed data (square markers), calculated profile (line) and difference plots for the Rietveld refinement of powder X-ray diffraction data of $PbPdO_2$. The short vertical markers represent allowed reflections.

3. Results and discussion

The powder X-ray diffraction profile of the $PbPdO_2$ sample is shown in Fig. 2 along with the fitted profile pattern calculated by Rietveld analysis. The initial lattice parameters and atomic positions for the refinement were taken from previously reported powder diffraction data by Meyer and Muller-Buschbaum [11]. No reflections, which cannot be indexed by this structure model were observed, and the phase homogeneity of the sample was confirmed. The refined crystallographic parameters are summarized in Table 1. The lattice parameters obtained from powder X-ray diffraction are a = 9.4547(1) Å, b = 5.45971(6) Å and c = 4.66051(6) Å in an orthorhombic cell. The Pb–O bond distance in $PbPdO_2$ is 2.325 Å, which is slightly larger than α-PbO (2.30 Å) [12]. The Pd–O bond distance in $PbPdO_2$ is 2.046 Å similar to that in other low dimensional palladium oxides such as Sr_2PdO_3 (1.992–2.068 Å) [5]. An interesting fact is that $PbPdO_2$ ex-

Table 1
Crystallographic parameters of $PbPdO_2$

Lattice parameters

Space group	*Imma* (74), orthorhombic
a (Å)	9.4547(1)
b (Å)	5.45971(6)
c (Å)	4.66051(6)
Unit cell volume (Å^3)	240.576(5)
Density (g/cm^3)	9.54235

Atomic parameters

Atom	Site	*x*	*y*	*z*
Pb	4*e*	0	1/4	0.7741(3)
Pd	4*c*	1/4	1/4	1/4
O	8*f*	0.345(1)	0	0

R_{wp} = 8.62%, R_I = 2.46%.

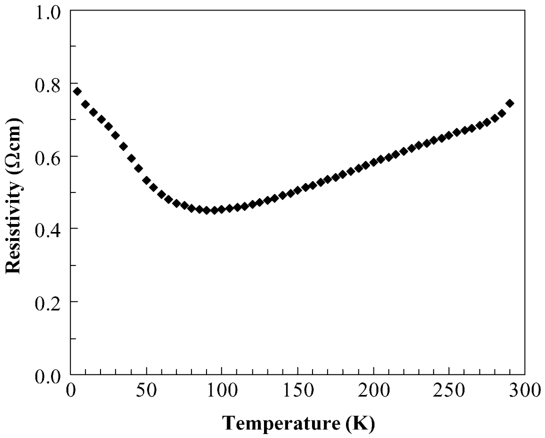

Fig. 3. Temperature-dependent dc resistivity of $PbPdO_2$.

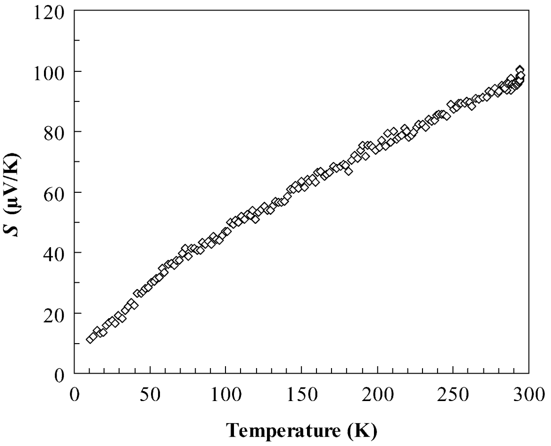

Fig. 5. Temperature-dependent thermoelectric power (*S*) of $PbPdO_2$.

hibits metallic conductivity as described below whereas both α-PbO and Sr_2PdO_3, which consist of the same structural sub-units as $PbPdO_2$, are insulators.

The temperature dependence of the electrical resistivity is shown in Fig. 3. It exhibits metal ($d\rho/dT > 0$) to insulator ($d\rho/dT < 0$) transition around 90 K. The temperature-dependent resistivity of $PbPdO_2$ between 90 and 300 has previously been reported by Watanabe and Nozaki [14]. Their results show similar metallic conductivity in this temperature range, and their resistivity values are in the same order as ours. In our studies, we also measured the resistivity below 90 K, and found that the resistivity increases below this temperature. Our attempt to fit this portion of the resistivity to the Arrhenius plot ($\rho = \rho_0 \exp[E_a/k_B T]$ where E_a is the activation energy) has failed; thus, the temperature dependence of the resistivity in this range is not likely to originate from suppression of carrier excitation over a band gap.

The temperature-dependent molar susceptibility is shown in Fig. 4. It exhibits a strong temperature dependence below 90 K where the transition from metal to insulator in the resistivity was also observed. The susceptibility data below 20 K were fitted to the Curie–Weiss law and the effective magnetic moment has been calculated. Based on the stoichiometric formula, $PbPdO_2$, the expected oxidation state of palladium is 2+. In the square planar crystal field, the highest filled orbital of Pd^{2+} is d_{xy}, and it is filled with a pair of spin up and down electrons. Thus, the expected effective spin magnetic moment is zero. However, the calculated value of the effective magnetic moment is $0.04\,\mu_B$/(formula unit). Since no secondary phase has been observed by powder X-ray diffraction, this result suggests that a small portion of palladium has the 1+ or 3+ oxidation state. One possibility for the valence shift is that there is small oxygen deficiency in the sample. In such a case, a small amount of Pd^+ is introduced, and a finite spin magnetic moment is expected from a spin unpaired electron in the $d_{x^2-y^2}$ orbital. A similar Curie behavior of the temperature-dependent susceptibility was also observed in other ternary palladium oxide systems such as $SrPd_3O_4$ [16]. From the low temperature region of the temperature-dependent magnetic susceptibility data, the concentration of Pd^+ has been estimated to be 1.82×10^{-4}/(formula unit). This amount corresponds to the number of localized charge carriers.

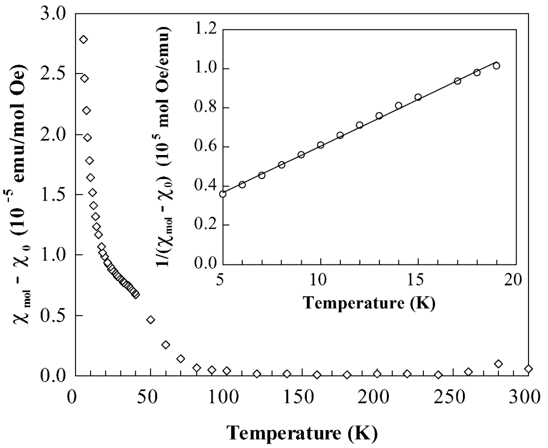

Fig. 4. Temperature dependence of residual susceptibility ($\chi - \chi_0$ where χ_0 is temperature-independent susceptibility) of $PbPdO_2$. The inset shows the inverse residual susceptibility fitted to the modified Curie-Weiss law, $\chi = C/(T - \theta_W) + \chi_0$, below 20 K.

The temperature-dependent thermoelectric power (*S*) is shown in Fig. 5. The sign of the thermoelectric power was positive for all temperatures indicating that the dominant charge carriers are holes. The thermoelectric power is roughly proportional to the temperature indicating that $PbPdO_2$ is essentially a metal as described by the Mott formula

$$S = \frac{\pi^2}{3}\frac{k_B^2 T}{e}\left(\frac{\delta \ln \sigma(E)}{\delta E}\right)_{E_F}$$

where E_F is the Fermi energy [17].

The temperature proportionality of the thermoelectric power has a transition around 80 K. This temperature is lower than metal–insulator transition exhibited in the resistivity measurement around 90 K. The thermoelectric power of $PbPdO_2$ at room temperature is quite large compared with conventional metals. Considering the order of charge carrier

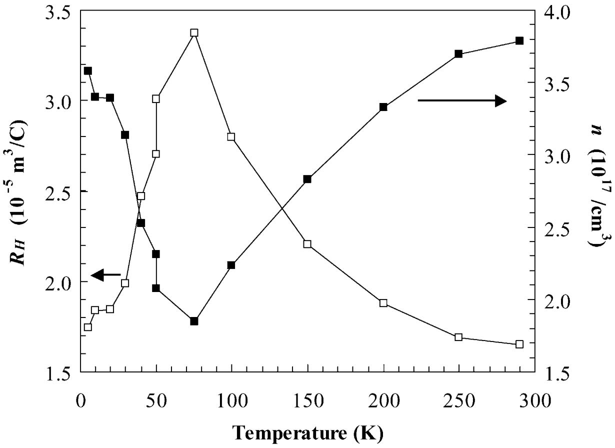

Fig. 6. Temperature-dependent Hall coefficients (R_H) and carrier density ($n = 1/eR_H$) of $PbPdO_2$.

concentration as described below and the large thermoelectric power, it is more like a semimetal possessing a deep pseudo-gap with a rather sharp band edge near the Fermi level. The thermoelectric power at 290 K is 95 μV/K, and it seems suitable for thermoelectric applications. However, the resistivity is quite high (0.75 Ω cm), and the power factor (S^2/ρ) of $PbPdO_2$ is quite small (0.012 μW/K^2 cm) compared with that of other metallic oxides having a large thermoelectric power such as $NaCo_2O_4$ (S = 13 μW/K^2 cm at 300 K) [4]. This large difference in the power factor between these compounds is mainly due to the high electrical resistivity of $PbPdO_2$, which it is a factor of 10^3 larger than $NaCo_2O_4$.

Hall effect measurement results are shown in Fig. 6. The Hall coefficients (R_H) are positive from 5 to 290 K indicating that the majority charge carriers are holes, consistent with the temperature-dependent thermoelectric power measurement results. In the figure, the carrier density (n) is estimated from the experimental data based on a single carrier model, $n = 1/eR_H$. The carrier density calculated in this model is in the same order ($\sim 10^{17}$ cm^{-3}) as semimetal materials such as bismuth [18]. The charge carrier concentration has a strong temperature dependence, and it has a maximum around 75 K. This temperature is close to the transition observed in the thermoelectric power.

The differences in transition temperatures among resistivity, magnetic susceptibility, thermoelectric power and Hall effect are not well understood. However, for all these properties, the transition is rather gradual; thus, it might be better to consider that these transitions are related and occur within a very broad transition region between 75 and 90 K. An intriguing feature of the temperature-dependent carrier density of $PbPdO_2$ is that the carrier density is smallest in this transition region where the electrical resistivity is smallest. Also, the carrier density at 5 K is 1.04×10^{-5}/(formula unit) and higher than that in the transition region contradicting the charge carrier localization indicated by Curie paramagnetism at low temperatures. These contradictions arise from the use of a single carrier model, and the relationship among temperature-dependent resistivity, magnetic susceptibility, thermoelectric power and Hall effect can more appropriately be rationalized by a two-band model. In the two-band model, different weights on charge carrier concentrations and mobility of holes and electrons contribute to electrical conductivity, thermoelectric power and Hall effect. For example, electrical conductivity is described as a summation of hole and electron contributions: $\sigma = q_h n_h \mu_h + q_e n_e \mu_e$ where q, n and μ are charge, charge carrier concentration and charge carrier mobility, respectively. In order to rationalize the physical property transitions, we assume that the electrical conduction is mainly contributed by electrons rather than holes. Because the majority charge carriers are holes as determined by the experiments, this assumption is allowed only if the electrons have higher mobility than holes. Above the transition region, the resistivity decrease ($d\rho/dT > 0$) is a normal metallic/semimetallic conductivity trend where scattering of carriers by thermal phonons are decreased as the temperature decreases. In addition, the increase in Hall coefficients above the transition region can be modeled by a decrease in the concentration of thermally excited holes. Below the transition region, the increase of the resistivity ($d\rho/dT < 0$) by the localization of charge carriers, which are assumed to be electrons, is manifested by the Curie tail of the temperature-dependent susceptibility. Due to the localization of electrons, the difference in charge carrier concentrations between holes and electrons increases; thus, the Hall coefficients decrease as long as there is no significant change in hole concentration. The broad kink of the thermoelectric power around 80 K is possibly caused by this change in relative charge carrier concentrations.

4. Conclusion

Single-phase polycrystalline samples of $PbPdO_2$ have been synthesized and resistivity, magnetic susceptibility, thermoelectric power and Hall coefficients have been measured. $PbPdO_2$ is essentially a metal. However, considering the large thermoelectric power and the difference between temperature-dependent thermoelectric power and Hall effects, it is rather a semimetal, and the majority of charge carriers are holes. It exhibits a metal–insulator transition around 90 K originating from the localization of charge carriers evidenced by the Curie paramagnetism at low temperatures. From a practical point of view, it would be interesting to explore the effect of carrier doping on the electrical resistivity and the thermoelectric power in order to achieve higher power factor in this system.

Acknowledgement

The work done at Aoyama Gakuin University was supported by The 21st Century COE program of the Ministry of Education, Culture, Sports, Science, and Technology, Japan and The Private School High-Tech Research Center Program of the Ministry of Education, Culture, Sports, Science, and Technology, Japan. We also thank Professor I. Terasaki for his helpful suggestions to the design of thermoelectric property measurement apparatus.

References

[1] J.G. Bednorz, K.A. Müller, Z. Phys. B 64 (1986) 189–193.
[2] Y. Maeno, H. Hashimoto, K. Yoshida, S. Nishizaki, T. Fujita, J.G. Bednorz, F. Lichtenberg, Nature 372 (1994) 532–534.
[3] K. Takada, H. Sakurai, E. Takayama-Muromachi, F. Izumi, R.A. Dilanian, T. Sasaki, Nature 422 (2003) 53–55.
[4] I. Terasaki, Y. Sasago, K. Uchinokura, Phys. Rev. B 56 (1997) R12685–R12687.
[5] Y. Nagata, T. Taniguchi, G. Tanaka, M. Satho, H. Samata, J. Alloy Compd. 346 (2002) 50–56.
[6] S.-J. Kim, S. Lemaux, G. Demazeau, J.-Y. Kim, J.-H. Choy, J. Am. Chem. Soc. 123 (2001) 10413–10414.
[7] S. Ichikawa, I. Terasaki, Phys. Rev. B 68 (2003) 2331011–2331014.
[8] C.M. Varma, Phys. Rev. Lett. 61 (1988) 2713–2716.
[9] A.W. Sleight, J.L. Gillson, P.E. Bierstedt, Solid State Commun. 17 (1975) 27–28.
[10] L.F. Mattheiss, E.M. Gyorgy, D.W. Johnson Jr., Phys. Rev. B. 37 (1988) 3745–3746.
[11] V.H. Meyer, H. Muller-Buschbaum, Z. Anorg. Chem. 442 (1978) 26–30.
[12] G. Trinquier, R. Hoffman, J. Phys. Chem. 88 (1984) 6696–6711.
[13] W.J. Moore, L. Pauling, J. Am. Chem. Soc. 63 (1941) 1392–1394.
[14] A. Watanabe, K. Nozaki, in Jpn. Kokai Tokkyo Koho, JP 06135723, Japan (1994).
[15] F. Izumi, T. Ikeda, Mater. Sci. Forum 321–324 (2000) 198–203.
[16] T. Taniguchi, Y. Nagata, T.C. Ozawa, M. Sato, Y. Noro, T. Uchida, H. Samata, J. Alloy Compd. 373 (2004) 67–72.
[17] N.F. Mott, H. Jones, Theory of the Properties of Metals and Alloys, Oxford University Press, Oxford, 1936, p. 311.
[18] C. Kittel, Introduction to Solid State Physics, 7th ed., Wiley, New York, 1996, p. 229.